PERGAMON

International Journal of Solids and Structures 37 (2000) 495–513

INTERNATIONAL JOURNAL OF SOLIDS and STRUCTURES

www.elsevier.com/locate/ijsolstr

Out-of-plane dynamic analysis of beams with arbitrarily varying curvature and cross-section by dynamic stiffness matrix method

C.S. Huang[a,*], Y.P. Tseng[b], S.H. Chang[b], C.L. Hung[b]

[a]*National Center for Research on Earthquake Engineering, 200, Sec. 3, Hsinhai Rd., Taipei, 106 Taiwan*
[b]*Department of Civil Engineering, Tamkang University, Tamsui, 25137 Taiwan*

Received 6 August 1998; in revised form 5 January 1999

Abstract

The first known dynamic stiffness matrix for noncircular curved beams with variable cross-section is developed, with which an exact solution of the out-of-plane free vibration of this type of beam is derived. By using the Laplace transform technique and the developed dynamic stiffness matrix and equivalent nodal force vector, the highly accurate dynamic responses, including the stress resultants, of the curved beams subjected to various types of loading can be easily obtained. The dynamic stiffness matrix and equivalent nodal force vector are derived based on the general series solution of the differential equations for the out-of-plane motion of the curved beams with arbitrary shapes and cross sections. The validity of the present solution for free vibration is demonstrated through comparison with published data. The accuracy of the present solution for transient response is also confirmed through comparison with the modal superposition solution for a simply-supported circular beam subjected to a moving load. With the proposed solution, both the free vibration and forced vibration of non-uniform parabolic curved beams with various ratios of rise to span are carried out. Nondimensional frequency parameters for the first five modes are presented in graphic form over a range of rise-to-span ratios ($0.05 \leq h/l \leq 0.75$) with different variations of the cross-section. Dynamic responses of the fixed–fixed parabolic curved beam subjected to a rectangular pulse are also presented for different rise-to-span ratios.

Keywords: Curved beams; Variable curvature and cross-section; Out-of-plane analysis; Dynamic stiffness method

* Corresponding author. Tel.: +886-2-27326607; fax: +886-2-27322223.
E-mail address: cshuang@email.ncree.gov.tw (C.S. Huang)

0020-7683/00/$ - see front matter
PII: S0020-7683(99)00017-7

1. Introduction

Like straight beams, curved beams (or arches) have found wide application in various industrial fields, such as spring design and aircraft structures in mechanical engineering, and the design of arch bridges and long-span roof in civil engineering. Research on the out-of-plane motion of curved beams (including rings) can be traced back to the nineteenth century (Michell, 1890; Love, 1892). As shown in the survey articles by Wagner and Ramamurti (1977), Markus and Nanasi (1981), Laura and Maurizi (1987), and Chidamparam and Leissa (1993), more than one hundred papers were devoted to studying the out-of-plane dynamic behaviors of planar curved beams. A number of curved elements have also been developed for the finite element approach (e.g., Choi and Lim, 1993; Koziey and Mirza, 1994; Litewka and Rakowski, 1997).

Various vibration problems for circular curved beams have been analyzed in the literature. Only a few investigated the dynamic responses for noncircular curved beams with variable cross sections even though this type of curved beam is quite often applied in civil engineering projects, such as arch bridges or elevated bridges. Irie et al. (1980a) appear to have been the first to investigate free vibrations of circular curved beams with variable cross-sections, using transfer matrix approach. Suzuki et al. (1983) developed a series solution for free vibrations of noncircular curved beams having variable cross-sections, in which symmetric modes and anti-symmetric modes were separately considered. Then, Suzuki et al. (1986) used the modal superposition technique to investigate the impulse responses of such curved beams. In the work of Suzuki et al. (1983, 1986), the effects of shear deformation and rotary inertia were neglected. Kawakami et al. (1995) proposed a numerical solution based on a discrete Green function and a numerical integral method for free vibrations of curved beams with variable cross sections. Apparently, the research work so far done on the dynamic responses of planar curved beams with variable cross-sections is not sufficient.

In this paper, we present a systematic approach to investigate the linear out-of-plane dynamic responses of planar curved beams with arbitrary shapes and cross-sections, which extends our work on uniform curved beams (Huang et al., 1998a) and in-plane dynamic responses (Huang et al., 1998b). In this study, the effects of shear deformation and rotary inertia are taken into account. The proposed approach combines the Laplace transform and dynamic stiffness method. The crucial step in this approach is to establish the dynamic stiffness matrix for curved beams with arbitrary shapes and cross sections, which is accomplished by using the Frobenius method (Hildebrand, 1976) to develop the series solution for such curved beams in terms of polynomials. This has not been done before.

By using the simple relationship between the transform parameters in Laplace transform and Fourier transform, one can easily transform the solution in the Laplace domain into the frequency domain. Then, the exact solution for the out-of-plane free vibration of a curved beam can be established. This exact solution is better than the series solution proposed by Suzuki et al. (1983) in two respects. The solutions for symmetric modes and anti-symmetric modes are not formulated separately, so our solution is not limited to problems with symmetry. Since the concept of dynamic stiffness matrix is adopted, convergent results are always guaranteed by increasing the number of solution terms or the number of elements. In order to obtain accurate results Suzuki et al. (1983) should use very high order polynomial terms, which frequently leads to numerical difficulties.

The use of Laplace transform makes it easy to obtain very accurate results for the transient responses without knowledge of the modal properties required by the normal mode method. Furthermore, the use of an analytical solution in the Laplace domain leads to high accuracy of the responses for the stress resultants, which usually requires hundreds of modes in the normal mode approach (Hung, 1998). Furthermore, in solving dynamic problems subjected to support excitations, which are often considered in earthquake engineering, no so called quasi-static solution as required in the normal mode approach is needed in the present solution.

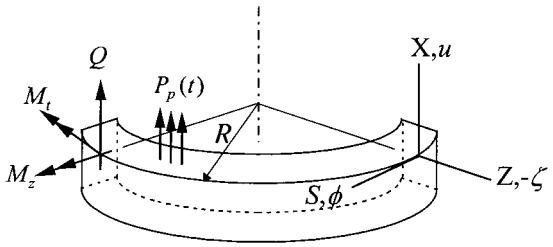

Fig. 1. Curved beam co-ordinates and displacement and stress resultants for out-of-plane motion.

To demonstrate the validity of our proposed solution for free vibration problems, a convergence study on a semi-elliptic curved beam with variable cross-sections is presented. The results are compared with those provided by Suzuki et al. (1986). Some numerical results for fixed–fixed parabolic arches with variable cross-sections, which are often designed for arch bridges, are given in graphic charts for a wide range of rise-to-span ratios. The proposed solution is compared with the modal superposition solution for a simply-supported circular curved beam subjected to a moving loading to exhibit the high accuracy of the present solution for transient analysis. Finally, a set of variable cross-section parabolic arches with various rise-to-span ratios subjected to a rectangular impulse are studied.

2. Mathematical formulation and solutions

Fig. 1 shows the adopted coordinate and a curved element where the bending moment, shear force, and twisting moment on the cross-section are denoted by M_z, Q, and M_t, respectively. The μ, ζ and ϕ represent the out-of-plane displacement, the bending rotation, and the twist angle of the centroidal axis, respectively. The positive directions for displacement components and stress resultants are also given in Fig. 1.

The dynamic equilibrium equations derived by using Hamilton's principle (e.g., Rao, 1971) in terms of the arc length coordinate S are as follows:

$$\frac{\partial Q}{\partial S} = \rho A\ddot{u} - P_p, \tag{1a}$$

$$-\frac{\partial M_z}{\partial S} + \frac{M_t}{R} + Q = \rho I_z\ddot{\zeta}, \tag{1b}$$

$$\frac{\partial M_t}{\partial S} + \frac{M_z}{R} = \rho J^*\ddot{\phi}, \tag{1c}$$

where A and J^*, respectively, are the area and polar moment of the cross section, ρ is the mass per unit volume, I_z is the second moment of the area of the cross section about the z-axis, and P_p is the external load. The derivative with respect to time is denoted by a dot.

The relationships of forces to displacements of a curved element are given by (e.g., Rao, 1971; Chidamparam and Leissa, 1993)

$$Q = \kappa GA\left(\frac{\partial u}{\partial S} - \zeta\right), \tag{2a}$$

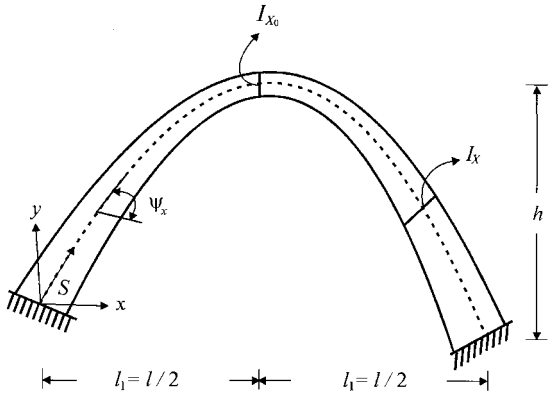

Fig. 2. Configuration of a parabolic arch with a variable cross-section.

$$M_z = -EI_z\left(\frac{\partial \zeta}{\partial S} + \frac{\phi}{R}\right), \tag{2b}$$

$$M_t = C\left(\frac{\partial \phi}{\partial S} - \frac{\zeta}{R}\right), \tag{2c}$$

where E and G are the Young's modulus and shear modulus, and κ and C are the shear coefficient and torsional stiffness coefficient of the cross section, respectively. The shear coefficient and torsional stiffness coefficient are dependent on the shape of the cross-section (Cowper, 1966; Timoshenko and Goodier, 1970). The effect of shear deformation is taken into account herein.

Substituting Eqs. (2a), (2b) and (2c) into the equilibrium equations (Eqs. (1a), (1b) and (1c)), and transforming the S coordinate into the Cartesian coordinate, x (see Fig. 2), one obtains the governing equation for the out-of-plane motion of a noncircular curved beam with a varying cross-section in a nondimensional form, as follows (Chang, 1997):

$$\bar{u}'' + \left(\frac{\xi'}{\xi} + \frac{\bar{A}'}{\bar{A}}\right)\bar{u}' - \frac{1}{\xi}\zeta' - \frac{\bar{A}'}{\bar{A}\xi}\zeta = \frac{\rho L^2}{E\lambda_1^2\xi^2}\ddot{\bar{u}} - \frac{L}{EA_0\bar{A}\lambda_1^2\xi^2}P_p, \tag{3a}$$

$$\zeta'' + \left(\frac{\xi'}{\xi} + \frac{\bar{I}_z'}{\bar{I}_z}\right)\zeta' - \left(\frac{\lambda_2^2\bar{C}}{\bar{R}^2\bar{I}_z\xi^2} + \frac{\lambda_1^2\bar{A}}{\bar{\gamma}_0^2\bar{I}_z\xi^2}\right)\zeta + \left(\frac{1}{\bar{R}\xi} + \frac{\lambda_2^2\bar{C}}{\bar{R}\bar{I}_z\xi}\right)\phi' - \left(\frac{\bar{R}'}{\xi\bar{R}^2} - \frac{\bar{I}_z'}{\bar{R}\bar{I}_z\xi}\right)\phi + \frac{\lambda_1^2\bar{A}}{\bar{\gamma}_0^2\bar{I}_z\xi}\bar{u}'$$
$$= \frac{\rho L^2}{E\xi^2}\ddot{\zeta}, \tag{3b}$$

$$\phi'' + \left(\frac{\xi'}{\xi} + \frac{\bar{C}'}{\bar{C}}\right)\phi' - \frac{1}{\lambda_2^2}\frac{\bar{I}_z}{\bar{R}^2\bar{C}\xi^2}\phi - \left(\frac{1}{\xi\bar{R}} + \frac{1}{\lambda_2^2}\frac{\bar{I}_z}{\bar{R}\bar{C}\xi}\right)\zeta' + \left(\frac{\bar{R}'}{\xi\bar{R}^2} - \frac{\bar{C}'}{\bar{R}\bar{C}\xi}\right)\zeta = \frac{\rho\lambda_3^2\bar{J}L^2}{E\lambda_2^2\xi^2\bar{C}}\ddot{\phi}, \tag{3c}$$

where the primes denote the derivatives with respect to $\bar{x}$. The following nondimensional quantities are introduced in Eqs. (3a), (3b) and (3c):

$$\bar{u} = \frac{u}{L}, \quad \bar{R} = \frac{R}{L}, \quad \bar{A}(\bar{x}) = \frac{A(\bar{x})}{A_0}, \quad \bar{I}_z(\bar{x}) = \frac{I_z(\bar{x})}{I_0}, \quad \bar{J}(\bar{x}) = \frac{J^*(\bar{x})}{J_0},$$

$$\bar{C}(\bar{x}) = \frac{C(\bar{x})}{C_0}, \quad \bar{\gamma}_0 = \frac{\gamma_0}{L} = \frac{\sqrt{I_0/A_0}}{L}, \quad \lambda_1^2 = \frac{\kappa G}{E}, \quad \lambda_2^2 = \frac{C_0}{EI_0},$$

$$\lambda_3^2 = \frac{J_0}{I_0}, \quad \xi = \frac{\mathrm{d}x}{\mathrm{d}S}, \quad \bar{x} = \frac{x}{L}, \tag{4}$$

where L is a representative length of the curved beam under consideration. The subscript '0' in Eq. (4) denotes the quantities at a reference cross-section, which is chosen as the middle cross-section in the following analysis. Eqs. (3a), (3b) and (3c) are a set of second order partial differential equations with non-constant coefficients.

To formulate the solution for Eqs. (3a), (3b) and (3c), the Laplace transform is carried out on these equations, and zero initial conditions are assumed. Then, the non-constant coefficients in Eqs. (3a), (3b) and (3c) are expressed in terms of their own Taylor's expansion series, which are given as:

$$\frac{\xi'}{\xi} + \frac{\bar{A}'}{\bar{A}} = \sum_{k=0}^{K} a_k(\bar{x}-\eta)^k, \quad \frac{1}{\xi} = \sum_{k=0}^{K} b_k(\bar{x}-\eta)^k, \quad \frac{\bar{A}'}{\bar{A}\xi} = \sum_{k=0}^{K} c_k(\bar{x}-\eta)^k,$$

$$\frac{1}{\xi^2} = \sum_{k=0}^{K} d_k(\bar{x}-\eta)^k, \quad \frac{\xi'}{\xi} + \frac{\bar{I}_z'}{\bar{I}_z} = \sum_{k=0}^{K} a_k^*(\bar{x}-\eta)^k,$$

$$\frac{\lambda_2^2\bar{C}}{\bar{R}^2\bar{I}_z\xi^2} + \frac{\lambda_1^2\bar{A}}{\bar{\gamma}_0^2\bar{I}_z\xi^2} = \sum_{k=0}^{K} b_k^*(\bar{x}-\eta)^k, \quad \frac{1}{\bar{R}\xi} + \frac{\lambda_2^2\bar{C}}{\bar{R}\bar{I}_z\xi} = \sum_{k=0}^{K} c_k^*(\bar{x}-\eta)^k,$$

$$\frac{\bar{R}'}{\xi\bar{R}^2} - \frac{\bar{I}_z'}{\bar{R}\bar{I}_z\xi} = \sum_{k=0}^{K} d_k^*(\bar{x}-\eta)^k, \quad \frac{\lambda_1^2\bar{A}}{\bar{\gamma}_0^2\bar{I}_z\xi} = \sum_{k=0}^{K} f_k^*(\bar{x}-\eta)^k,$$

$$\frac{\xi'}{\xi} + \frac{\bar{C}'}{\bar{C}} = \sum_{k=0}^{K} \bar{a}_k(\bar{x}-\eta)^k, \quad \frac{\bar{I}_z}{\lambda_2^2\bar{R}^2\bar{C}\xi^2} = \sum_{k=0}^{K} \bar{b}_k(\bar{x}-\eta)^k,$$

$$\frac{1}{\bar{R}\xi} + \frac{\bar{I}_z}{\lambda_2^2\bar{R}\bar{C}\xi} = \sum_{k=0}^{K} \bar{c}_k(\bar{x}-\eta)^k, \quad \frac{\bar{R}'}{\xi\bar{R}^2} - \frac{\bar{C}'}{\bar{R}\bar{C}\xi} = \sum_{k=0}^{K} \bar{d}_k(\bar{x}-\eta)^k, \quad \frac{\bar{J}}{\bar{C}\xi^2} = \sum_{k=0}^{K} \bar{f}_k(\bar{x}-\eta)^k. \tag{5}$$

In terms of polynomials, expressing the loading function $P_p(\bar{x},t)$ and the displacement components $\bar{u}(\bar{x},t)$, $\xi(\bar{x},t)$ and $\phi(\bar{x},t)$ after the Laplace transform that are, respectively, denoted as $\tilde{P}_p(\bar{x},\tilde{s})$, $\tilde{U}(\bar{x},\tilde{s})$, $\tilde{Z}(\bar{x},\tilde{s})$ and $\tilde{\Phi}(\bar{x},\tilde{s})$, where $\tilde{s}$ is the Laplace transform parameter, one obtains

$$\frac{L}{E\lambda_1^2 A_0\bar{A}\xi^2}\tilde{P}_p = \sum_{k=0}^{K} p_k(\bar{x}-\eta)^k, \tag{6}$$

$$\tilde{\bar{U}} = \sum_{j=0}^{J} A_j(\bar{x}-\eta)^j, \quad \tilde{Z} = \sum_{j=0}^{J} B_j(\bar{x}-\eta)^j, \quad \tilde{\Phi} = \sum_{j=0}^{J} D_j(\bar{x}-\eta)^j. \tag{7}$$

It should be noted that the coefficients of the polynomials in Eqs. (6) and (7) are dependent on $\tilde{s}$. As long as the loading function and the geometry of the curved beam under consideration are defined, their Taylor's expansion series given in Eqs. (5) and (6) can be obtained with the aid of a symbolic computation system such as "*Mathematica*", "*MACSYMA*" or "*MATLAB*".

Substituting Eqs. (5)–(7) into the Laplace transformed equations (Eqs. (3a), (3b) and (3c)), one can establish the following recursive formulas for the coefficients for the displacement components given in Eq. (7):

$$A_{j+2} = \frac{-1}{(j+1)(j+2)}\left\{\sum_{k=0}^{j}\left[(k+1)a_{j-k}A_{k+1} - (k+1)b_{j-k}B_{k+1} - \frac{\rho\tilde{s}^2L^2}{E\lambda_1^2}d_{j-k}A_k - c_{j-k}B_k\right] + p_j\right\}, \tag{8a}$$

$$B_{j+2} = \frac{-1}{(j+1)(j+2)}\sum_{k=0}^{j}\left[(k+1)f^*_{j-k}A_{k+1} + (k+1)a^*_{j-k}B_{k+1} + (k+1)c^*_{j-k}D_{k+1} - \left(b^*_{j-k} + \frac{\rho\tilde{s}^2L^2}{E}d_{j-k}\right)B_k - d^*_{j-k}D_k\right] \tag{8b}$$

$$D_{j+2} = \frac{-1}{(j+1)(j+2)}\sum_{k=0}^{j}\left[-(k+1)\bar{c}_{j-k}B_{k+1} + (k+1)\bar{a}_{j-k}D_{k+1} + \bar{d}_{j-k}B_k - \left(\bar{b}_{j-k} + \frac{\rho L^2\lambda_3^2\tilde{s}^2}{E\lambda_2^2}\bar{f}_{j-k}\right)D_k\right], \tag{8c}$$

where $j = 0, 1, 2, 3,....$

The recursive formulae relate the coefficients for $j \geq 2$ in Eq. (7) to A_0, A_1, B_0, B_1, D_0 and D_1. As a result, the solution given in Eq. (7) can be further modified and simply expressed as

$$\tilde{\bar{U}}(\bar{x}) = A_0\tilde{\bar{u}}_0(\bar{x}) + A_1\tilde{\bar{u}}_1(\bar{x}) + B_0\tilde{\bar{u}}_2(\bar{x}) + B_1\tilde{\bar{u}}_3(\bar{x}) + D_0\tilde{\bar{u}}_4(\bar{x}) + D_1\tilde{\bar{u}}_5(\bar{x}) + \tilde{\bar{u}}_p(\bar{x}), \tag{9a}$$

$$\tilde{Z}(\bar{x}) = A_0\tilde{\zeta}_0(\bar{x}) + A_1\tilde{\zeta}_1(\bar{x}) + B_0\tilde{\zeta}_2(\bar{x}) + B_1\tilde{\zeta}_3(\bar{x}) + D_0\tilde{\zeta}_4(\bar{x}) + D_1\tilde{\zeta}_5(\bar{x}) + \tilde{\zeta}_p(\bar{x}) \tag{9b}$$

$$\tilde{\Phi}(\bar{x}) = A_0\tilde{\phi}_0(\bar{x}) + A_1\tilde{\phi}_1(\bar{x}) + B_0\tilde{\phi}_2(\bar{x}) + B_1\tilde{\phi}_3(\bar{x}) + D_0\tilde{\phi}_4(\bar{x}) + D_1\tilde{\phi}_5(\bar{x}) + \tilde{\phi}_p(\bar{x}), \tag{9c}$$

where $\tilde{\bar{u}}_i$, $\tilde{\zeta}_i$ and $\tilde{\phi}_i$ ($i = 1, 2,..., 5$, and p) are polynomial functions with coefficients determined from Eqs. (8a), (8b) and (8c). The first six terms in each of Eqs. (9a), (9b) and (9c) construct the set of the general homogeneous solutions for Eqs. (3a), (3b) and (3c) in the Laplace domain, whereas the last term represents the particular solution.

3. Dynamic stiffness matrix and loading vector

If one directly applies the solution form given in Eqs. (9a), (9b) and (9c), one needs to use very high order polynomials to obtain accurate results. This seems to be theoretically feasible, but numerical difficulties are often encountered, as reported by Suzuki et al. (1983). Furthermore, one may also face a theoretically fatal limit which the convergent radius of the solution given by Eqs. (9a), (9b) and (9c) may not cover the whole space domain under consideration. To overcome these drawbacks and make the solution more applicable to a wide class of problems, the concept of the dynamic stiffness matrix is adopted here.

By using Eqs. (9a), (9b) and (9c), the nodal displacement components of a curved element, say the n-th element, (see Fig. 3) can be expressed as

$$\begin{Bmatrix} \tilde{U}_0 \\ \tilde{Z}_0 \\ \tilde{\Phi}_0 \\ \tilde{U}_1 \\ \tilde{Z}_1 \\ \tilde{\Phi}_1 \end{Bmatrix}_n = [\tilde{N}]_n \begin{Bmatrix} A_0 \\ A_1 \\ B_0 \\ B_1 \\ D_0 \\ D_1 \end{Bmatrix} + \begin{Bmatrix} \tilde{u}_p(\bar{x}_n) \\ \tilde{\zeta}_p(\bar{x}_n) \\ \tilde{\phi}_p(\bar{x}_n) \\ \tilde{u}_p(\bar{x}_{n+1}) \\ \tilde{\zeta}_p(\bar{x}_{n+1}) \\ \tilde{\phi}_p(\bar{x}_{n+1}) \end{Bmatrix}, \tag{10}$$

where

$$[\tilde{N}]_n = \begin{bmatrix} [\tilde{\beta}]|_{\bar{x}=\bar{x}_n} \\ [\tilde{\beta}]|_{\bar{x}=\bar{x}_{n+1}} \end{bmatrix}_n, \tag{11a}$$

$$[\tilde{\beta}] = \begin{bmatrix} \tilde{u}_0(\bar{x}) & \tilde{u}_1(\bar{x}) & \tilde{u}_2(\bar{x}) & \tilde{u}_3(\bar{x}) & \tilde{u}_4(\bar{x}) & \tilde{u}_5(\bar{x}) \\ \tilde{\zeta}_0(\bar{x}) & \tilde{\zeta}_1(\bar{x}) & \tilde{\zeta}_2(\bar{x}) & \tilde{\zeta}_3(\bar{x}) & \tilde{\zeta}_4(\bar{x}) & \tilde{\zeta}_5(\bar{x}) \\ \tilde{\phi}_0(\bar{x}) & \tilde{\phi}_1(\bar{x}) & \tilde{\phi}_2(\bar{x}) & \tilde{\phi}_3(\bar{x}) & \tilde{\phi}_4(\bar{x}) & \tilde{\phi}_5(\bar{x}) \end{bmatrix}. \tag{11b}$$

It should be noted that real displacement, instead of nondimensional displacement, is used in Eq. (10) such that $\tilde{u}_i = L\tilde{u}$ ($i = 0, 1, 2,..., 5$, and p).

Using Eqs. (2a), (2b) and (2c) and Eqs. (10), (11a) and (11b), one can express the nodal stress resultants in terms of nodal displacement components in the Laplace domain as

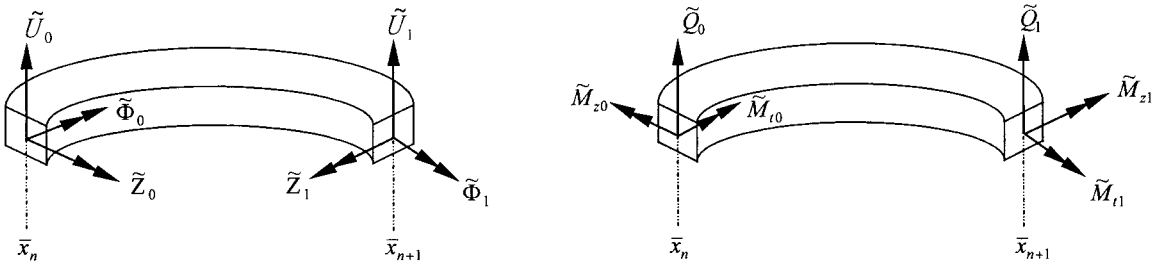

Fig. 3. Positive displacement and stress resultant for the n-th element.

$$\begin{Bmatrix} \tilde{Q}_0 \\ \tilde{M}_{z0} \\ \tilde{M}_{t0} \\ \tilde{Q}_1 \\ \tilde{M}_{z1} \\ \tilde{M}_{t1} \end{Bmatrix}_n = [\tilde{k}]_n \begin{Bmatrix} \tilde{U}_0 \\ \tilde{Z}_0 \\ \tilde{\Phi}_0 \\ \tilde{U}_1 \\ \tilde{Z}_1 \\ \tilde{\Phi}_1 \end{Bmatrix}_n + \left\{\tilde{f}_p\right\}_n, \tag{12}$$

where

$$[\tilde{k}]_n = (EI_{z0})\left([\tilde{\Gamma}_1]_n + [\tilde{\Gamma}_2]_n\right)[\tilde{N}]_n^{-1}, \tag{13a}$$

$$\left\{\tilde{f}_p\right\}_n = -[\tilde{k}]_n \begin{Bmatrix} \{\tilde{r}_p\}_n\big|_{\bar{x}=\bar{x}_n} \\ \{\tilde{r}_p\}_n\big|_{\bar{x}=\bar{x}_{n+1}} \end{Bmatrix} + EI_0 \begin{Bmatrix} \{\tilde{\sigma}_p\}_n\big|_{\bar{x}=\bar{x}_n} \\ -\{\tilde{\sigma}_p\}_n\big|_{\bar{x}=\bar{x}_{n+1}} \end{Bmatrix}, \tag{13b}$$

$$[\tilde{\Gamma}_1]_n = [\Lambda_1]_n \begin{bmatrix} \dfrac{\partial}{\partial \bar{x}}[\tilde{\beta}]_n\Big|_{\bar{x}=\bar{x}_n} \\ \dfrac{\partial}{\partial \bar{x}}[\tilde{\beta}]_n\Big|_{\bar{x}=\bar{x}_{n+1}} \end{bmatrix}, \tag{13c}$$

$$[\tilde{\Gamma}_2]_n = [\Lambda_2]_n \begin{bmatrix} [\tilde{\alpha}]_n\big|_{\bar{x}=\bar{x}_n} \\ [\tilde{\alpha}]_n\big|_{\bar{x}=\bar{x}_{n+1}} \end{bmatrix}, \tag{13d}$$

$$[\tilde{\alpha}]_n = \begin{bmatrix} \tilde{\xi}_0(\bar{x}) & \tilde{\xi}_1(\bar{x}) & \tilde{\xi}_2(\bar{x}) & \tilde{\xi}_3(\bar{x}) & \tilde{\xi}_4(\bar{x}) & \tilde{\xi}_5(\bar{x}) \\ \tilde{\phi}_0(\bar{x}) & \tilde{\phi}_1(\bar{x}) & \tilde{\phi}_2(\bar{x}) & \tilde{\phi}_3(\bar{x}) & \tilde{\phi}_4(\bar{x}) & \tilde{\phi}_5(\bar{x}) \\ \tilde{\zeta}_0(\bar{x}) & \tilde{\zeta}_1(\bar{x}) & \tilde{\zeta}_2(\bar{x}) & \tilde{\zeta}_3(\bar{x}) & \tilde{\zeta}_4(\bar{x}) & \tilde{\zeta}_5(\bar{x}) \end{bmatrix}_n, \tag{13e}$$

$$\{\tilde{r}_p\}_n = \left(\tilde{u}_p(\bar{x})\ \tilde{\zeta}_p(\bar{x})\ \tilde{\phi}_p(\bar{x})\right)_n^T \tag{13f}$$

and

$$\{\tilde{\sigma}_p\}_n = \begin{Bmatrix} -\dfrac{\lambda_1^2 \bar{A}(\bar{x})}{\gamma_0^2}\left[\dfrac{\xi(\bar{x})\tilde{u}_p'(\bar{x})}{L} - \tilde{\zeta}_p(\bar{x})\right] \\ \dfrac{\bar{I}_z(\bar{x})}{L}\left[\xi(\bar{x})\tilde{\zeta}_p'(\bar{x}) + \dfrac{\tilde{\phi}_p(\bar{x})}{\bar{R}(\bar{x})}\right] \\ -\dfrac{\lambda_2^2 \bar{C}(\bar{x})}{L}\left[\xi(\bar{x})\tilde{\phi}_p'(\bar{x}) - \dfrac{\tilde{\zeta}_p(\bar{x})}{\bar{R}(\bar{x})}\right] \end{Bmatrix}_n. \tag{13g}$$

The matrices $[\Lambda_1]_n$ and $[\Lambda_2]_n$ are diagonal with the diagonal vectors equal to

$$\left(-\frac{\lambda_1^2}{\gamma_0^2 L}\bar{A}(\bar{x}_n)\xi(\bar{x}_n),\quad \frac{\bar{I}_z(\bar{x}_n)\xi(\bar{x}_n)}{L},\quad -\frac{\lambda_2^2\bar{C}(\bar{x}_n)\xi(\bar{x}_n)}{L},\quad \frac{\lambda_1^2}{\gamma_0^2 L}\bar{A}(\bar{x}_{n+1})\xi(x_{n+1}),\quad -\frac{\bar{I}_z(\bar{x}_{n+1})\xi(\bar{x}_{n+1})}{L},\right.$$

$$\left.\frac{\lambda_2^2\bar{C}(\bar{x}_{n+1})\xi(\bar{x}_{n+1})}{L}\right)$$

and

$$\left(\frac{\lambda_1^2}{\gamma_0^2}\bar{A}(\bar{x}_n),\quad \frac{\bar{I}_z(\bar{x}_n)}{\bar{R}(\bar{x}_n)L},\quad \frac{\lambda_2^2\bar{C}(\bar{x}_n)}{\bar{R}(\bar{x}_n)L},\quad -\frac{\lambda_1^2}{\gamma_0^2}\bar{A}(\bar{x}_{n+1}),\quad -\frac{\bar{I}_z(\bar{x}_{n+1})}{\bar{R}(\bar{x}_{n+1})L},\quad -\frac{\lambda_2^2\bar{C}(\bar{x}_{n+1})}{\bar{R}(\bar{x}_{n+1})L}\right),$$

respectively. It should be mentioned that $[\tilde{k}]_n$ is the so-called dynamic stiffness matrix for the n-th curved element, which includes the effect of inertia forces, and $\{\tilde{f}_p\}_n$ is the equivalent nodal external loading, which is transformed from the distributed load in an element.

Like the finite element approach, the continuity conditions between adjacent elements result in assembling the dynamic stiffness matrices for all the elements to form a global dynamic matrix, $[\tilde{K}]$, such that

$$[\tilde{K}]\{\tilde{U}\} = \{\tilde{F}\}, \tag{14}$$

where $\{\tilde{U}\}$ is the nodal displacement vector for the curved beam system under consideration while $\{F\}$ is the equivalent external loading vector applied at the ends of each element. Then, the unknown nodal displacement components in the Laplace domain can be obtained by solving the set of linear algebraic equations given by Eq. (14).

A convergent solution is always guaranteed, which can be obtained either by increasing the number of solution terms, J in Eq. (7), and the number of terms for geometric functions and loading function, K in Eqs. (5) and (6), or by increasing the number of elements. This is similar to combining h- and p-refinement in the finite element approach. It should be noted that each polynomial function in Eqs. (9a), (9b) and (9c) includes J polynomial terms. In the present procedure, the number of J for each element is determined by controlling the relative and the absolute errors for each polynomial function in Eqs. (9a), (9b) and (9c). The number of elements is controlled by the magnitude ratios of a polynomial function to each of its polynomial terms for each element. When the minimum ratio is less than 10^{-8}, the element is refined in order to avoid loss of accuracy in the numerical operation by using double precision (15 or 16 significant digits). If one uses double precision on a super-computer, one can use a control value much smaller than 10^{-8}.

4. Free vibration analysis

To perform a free vibration analysis, one can replace the Laplace transform parameter $\tilde{s}$ in the previous solution formulation with $\mathrm{i}\omega$, where $\mathrm{i} = \sqrt{-1}$, and neglect the particular solution parts. Consequently, one can rewrite Eq. (14) as

$$\begin{bmatrix} \begin{bmatrix}\tilde{K}_{\mathrm{uu}}\end{bmatrix} & \begin{bmatrix}\tilde{K}_{\mathrm{ub}}\end{bmatrix} \\ \begin{bmatrix}\tilde{K}_{\mathrm{bu}}\end{bmatrix} & \begin{bmatrix}\tilde{K}_{\mathrm{bb}}\end{bmatrix} \end{bmatrix} \begin{Bmatrix} \{\tilde{U}_{\mathrm{u}}\} \\ \{\tilde{U}_{\mathrm{b}}\} \end{Bmatrix} = \begin{Bmatrix} \{0\} \\ \{\tilde{F}_{\mathrm{b}}\} \end{Bmatrix}, \tag{15}$$

where $\{\tilde{U}_{\mathrm{u}}\}$ corresponds to the unknown vibratory displacement components at the nodal points, $\{\tilde{U}_{\mathrm{b}}\}$ is the prescribed vibratory displacement components on the boundaries, and $\{\tilde{F}_{\mathrm{b}}\}$ is the unknown

vibratory stress resultants on the displacement prescribed boundaries. Because $\{\tilde{U}_b\}$ is usually a zero vector in a free vibration problem, the natural frequencies for the curved beams are those ω's resulting in the zero determinant of $[\tilde{K}_{uu}]$. It should be noted that the solution is an exact solution because no approximation is made.

4.1. Convergence study

In order to assess the validity of the proposed solution, a convergence study was carried out on a fixed–fixed semi-elliptic curved beam with a varying cross-section, and a comparison was made with the results given by Suzuki et al. (1986). The curved beam under consideration, which has a circular cross-section, is shown in Fig. 4. The variation of the diameter of the cross-section is described by $d(\psi) = d_c(1 + 0.2\psi^2)$, where d_c is the diameter at the middle and is set equal to 6 meters, and ψ is the angle between the tangent at the eccentric angle of an ellipse (θ) equal to zero and that at any point on the center line (see Fig. 4). Poisson's ratio was set equal to 0.3 for all numerical results shown in this paper.

Tables 1 and 2 list the first six natural frequency parameters, $\omega^2 L^4 (\rho A_0/EI_0)^{1/4}$, obtained by using 8 and 16 elements, respectively, with different numbers of solution terms, J in Eq. (7), and geometric terms, K in Eq. (5). It should be noted that L is set equal to $\sqrt{a^2 + b^2}$. Indeed, the data show that the convergent results can be obtained by increasing the number of elements or by increasing K and J at the same time. As expected, a larger number of elements cooperating with smaller numbers of K and J can provide a convergent solution. Comparing these with the results given by Suzuki et al. (1986) reveals that our convergent results are slightly smaller than theirs, which is mainly because the effects of shear deformation and rotary inertia were neglected in their work.

Table 3 shows a comparison between the convergent results from the proposed solution and those provided by Irie et al. (1980b) for a fixed–fixed circular beam with a uniform cross-section. The circular beam has an opening angle equal to 80° and $\sqrt{AR^2/I_z} = 20$. Solving the same type of governing equations, our results were obtained by setting twenty solution terms and one geometric term with two elements while Irie et al. (1980b) used the transfer matrix method. These results are exactly the same if four significant figures are considered.

4.2. Numerical results

To fill the void in the available data on a parabolic arch with a varying cross-section, we studied fixed–fixed parabolic arches with varying height of the rectangular cross-section (see Fig. 2) such that

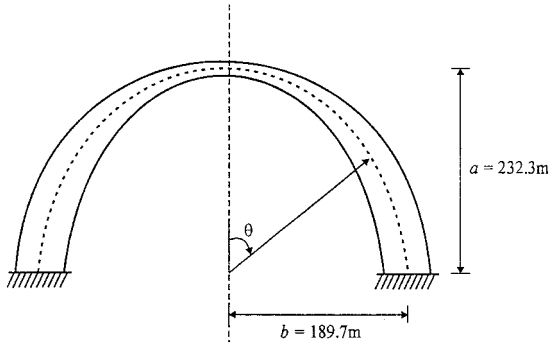

Fig. 4. Sketch of a semi-elliptic curved beam with a varying cross-section.

Table 1
Convergence of frequency parameters $(\omega^2 L^4 \rho A_0/EI_0)^{1/4}$ for a semi-elliptic curved beam with a varying cross-section using 8 elements

Mode	$(K+1)$ in Eq. (5)	$(J+1)$ in Eq. (7)			Suzuki et al. (1986)
		10	20	30	
1	10	1.71085	1.71088	1.71088	1.71129
	15	1.71085	1.71087	1.71087	
2	10	2.66358	2.66354	2.66354	2.66503
	15	2.66358	2.66353	2.66353	
3	10	3.72848	3.72850	3.72850	3.73248
	15	3.72848	3.72849	3.72849	
4	10	4.81629	4.81585	4.81585	4.82413
	15	4.81629	4.81584	4.81584	
5	10	5.90675	5.90647	5.90646	5.92170
	15	5.90675	5.90646	5.90646	
6	10	6.99516	6.99429	6.99427	7.01825
	15	6.99516	6.99427	6.99427	

$$I_X(x) = \frac{I_{X0}}{\left[1-(1-\eta^*)\dfrac{|x-l_1|}{l_1}\right]\cos\psi_x}, \tag{16}$$

where l_1 is half of the span length l and ψ_x is the angle between the tangent at any point on the centroidal axis and a horizontal axis. The value of the constant η^* is between 0 and 1, with larger η^* indicating smaller variation of the cross-section from the middle to the ends. This type of parabolic arch is designed quite often in civil engineering projects (Hu, 1988). It should be noted that the presented results are for a rectangular cross-section with a height-to-width ratio equal to 0.5 and $\bar{\gamma}_0 = 0.01$ at the middle. The span length l is chosen as the characteristic length L.

Table 2
Convergence of frequency parameters $(\omega^2 L^4 \rho A_0/EI_0)^{1/4}$ for a semi-elliptic curved beam with a varying cross-section using 16 elements

Mode	$(K+1)$ in Eq. (5)	$(J+1)$ in Eq. (7)			Suzuki et al. (1986)
		10	20	30	
1	10	1.71087	1.71087	1.71087	1.71129
	15	1.71087	1.71087	1.71087	
2	10	2.66353	2.66353	2.66353	2.66503
	15	2.66353	2.66353	2.66353	
3	10	3.72849	3.72849	3.72849	3.73248
	15	3.72849	3.72849	3.72849	
4	10	4.81584	4.81584	4.81584	4.82413
	15	4.81584	4.81584	4.81584	
5	10	5.90646	5.90646	5.90646	5.92170
	15	5.90646	5.90646	5.90646	
6	10	6.99428	6.99427	6.99427	7.01825
	15	6.99428	6.99427	6.99427	

Table 3
Comparison of nondimensional frequency parameters $[(\omega^2 R^4(\rho A/EI_z))^{1/4}]$ for a circular beam obtained using different methods

Mode	$(\omega^2 R^4(\rho A/EI_z))^{1/4}$	
	Present	Irie et al. (1980b)
1	3.13412	3.134
2	5.02223	5.022
3	5.58418	5.584
4	6.73358	6.734

Fig. 5(a,b) show the variation of the frequency parameters $\omega l^2(\rho A_0/EI_0)^{1/2}$ with h/l for $\eta^* = 0.25$, 0.5, 0.75 and 1, where h is the height of the parabolic arch under consideration. The frequency parameters increase as η^* decreases, which indicates that the increase of the stiffness is larger than the increase of the mass of the beam when η^* is decreasing. This is similar to observations for in-plane vibration (Huang et al., 1998c). However, the frequency parameters are not very sensitive to the change of η^* except for higher modes with small h/l. The frequency parameters also decrease with the increase of h/l except for higher modes with small h/l, which is somewhat different from the behavior for in-plane vibration (Huang et al., 1998c). There is modal crossing for the second anti-symmetric mode and the third symmetric mode when h/l is less than 0.2, which indicates the possibility of one frequency corresponding to two modes for certain values of h/l.

5. Transient analysis

To perform transient analysis, one needs to carry out the inverse of Laplace transform after obtaining the solution for the displacement components and stress resultants at the desired positions in the Laplace domain by applying the formulation in preceding sections. The efficient numerical technique developed by Durbin (1974) is adopted here and is combined with the fast Fourier transform technique to accelerate the computation. The advantages of Durbin's scheme over others were investigated by Narayanan and Beskos (1982). The procedure for computation implementation has been described in detail by Huang et al. (1996), which will not recapitulated here.

5.1. Accuracy of the solution

To confirm the high accuracy of the proposed solution, a comparison is made with the normal mode solution for a simply supported uniform circular curved beam subjected to a moving loading with constant magnitude and speed. For a circular curved beam with boundary conditions of zero out-of-plane displacement u, twist angle ϕ, and bending moment M_z at the ends, it is easy to obtain the natural frequency and mode shapes in terms of a closed form solution (Hung, 1998). The geometrical properties of the curved beam with square cross-section under consideration are $R = 50$ m, opening angle $= 30^\circ$ and $1/\bar{\gamma}_0 = 70$. The material properties are Poisson's ratio $= 0.3$ and $\sqrt{E/\rho} = 3000$ m/sec. The loading function is defined as

$$P_p(t) = p_0\delta(S - vt), \tag{17}$$

where p_0 is set equal to EA_0/R in this case, and v is the moving velocity of the load. It should be noted that the characteristic length (L) is set equal to R.

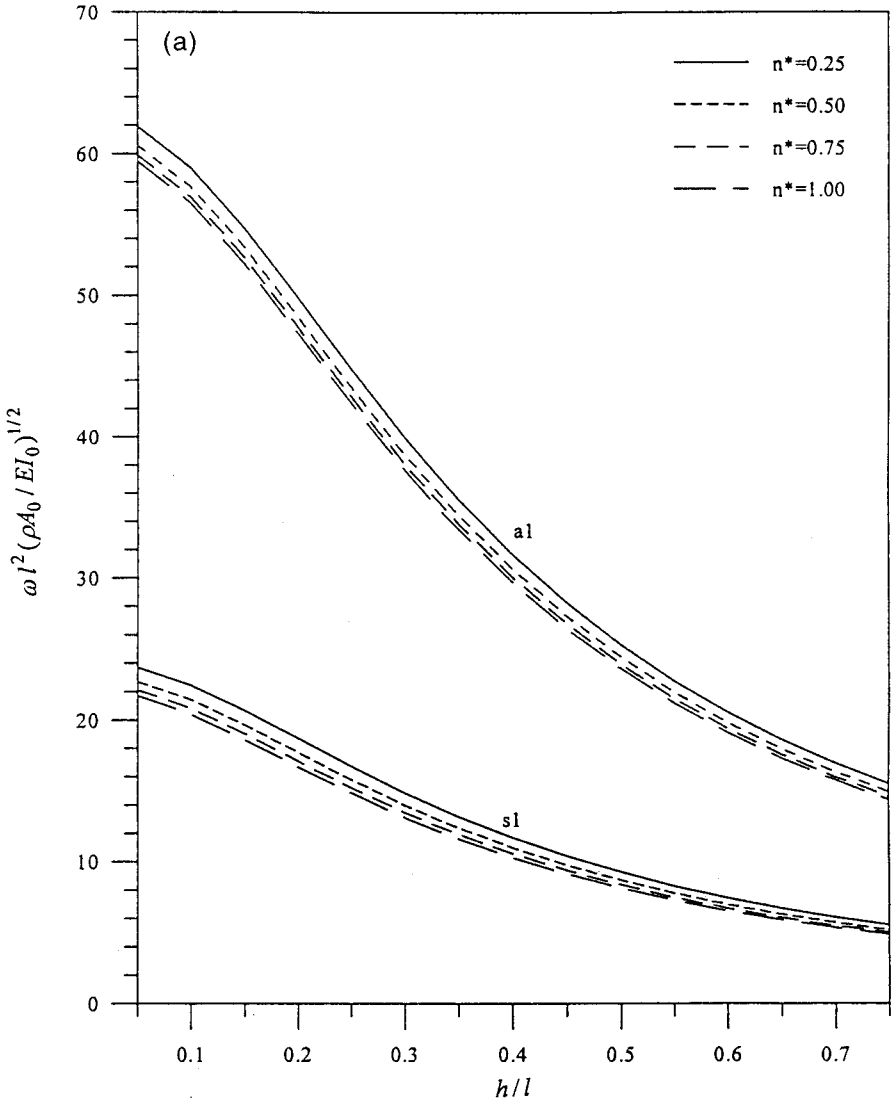

Fig. 5. (a) Variation of $\omega l^2\sqrt{\rho A_0/EI_0}$ with h/l for fixed–fixed parabolic arches with $\bar{\gamma}_0 = 0.01$ (1st symmetric and anti-symmetric modes); (b) Variation of $\omega l^2\sqrt{\rho A_0/EI_0}$ with h/l for fixed–fixed parabolic arches with $\bar{\gamma}_0 = 0.01$ (2nd and 3rd symmetric modes and 2nd anti-symmetric mode).

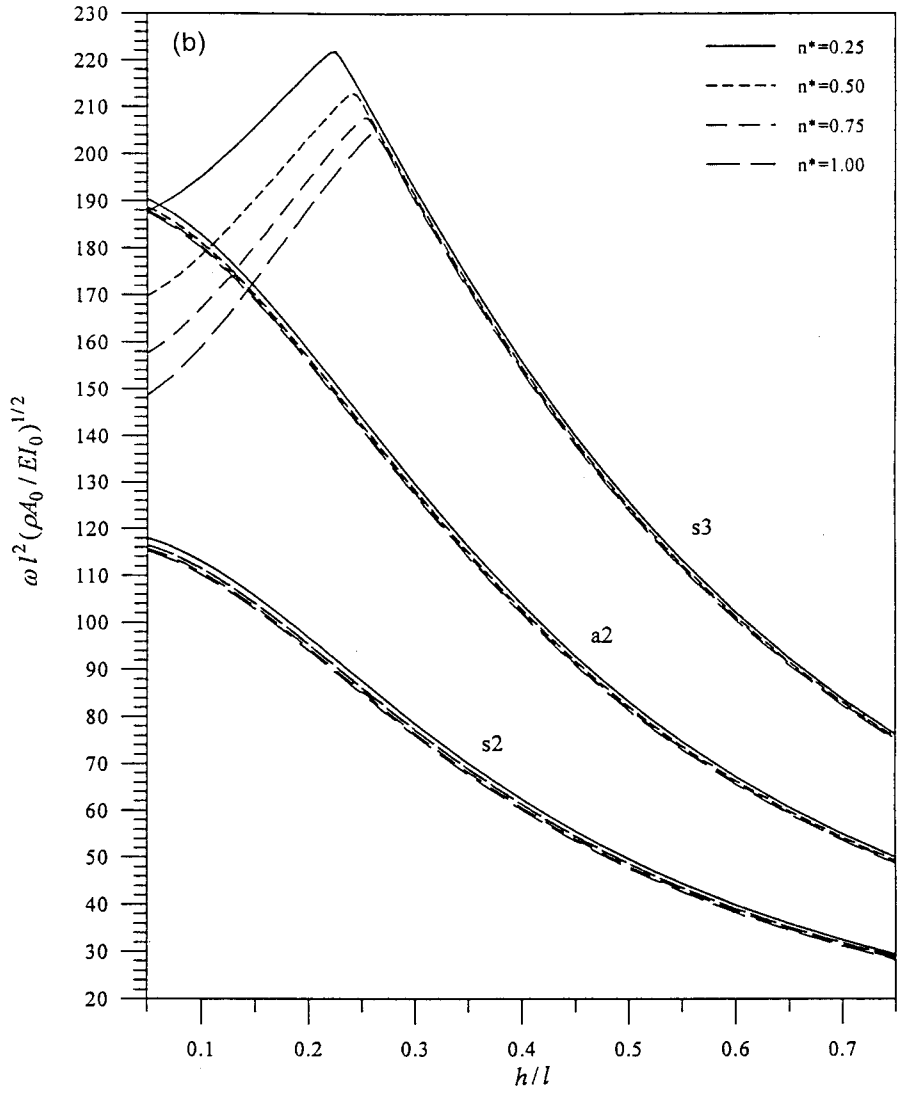

Fig. 5 (*continued*).

The following nondimensional stress resultants are introduced for the numerical results shown herein:

$$Q^* = \frac{Q}{\kappa G A_0}, \quad M_z^* = \frac{M_z L}{E I_0}, \quad M_t^* = \frac{M_t L}{C_0}. \tag{18}$$

The response histories for $\bar{u}$, Q^* and M_z^* at the middle of the beam are shown in Fig. 6, in which l_c is defined as being equal to the total arc length. The numbers of modes used to obtain the maximum responses with four-significant-figure convergence (expect for Q^*) are given in parentheses. As can be

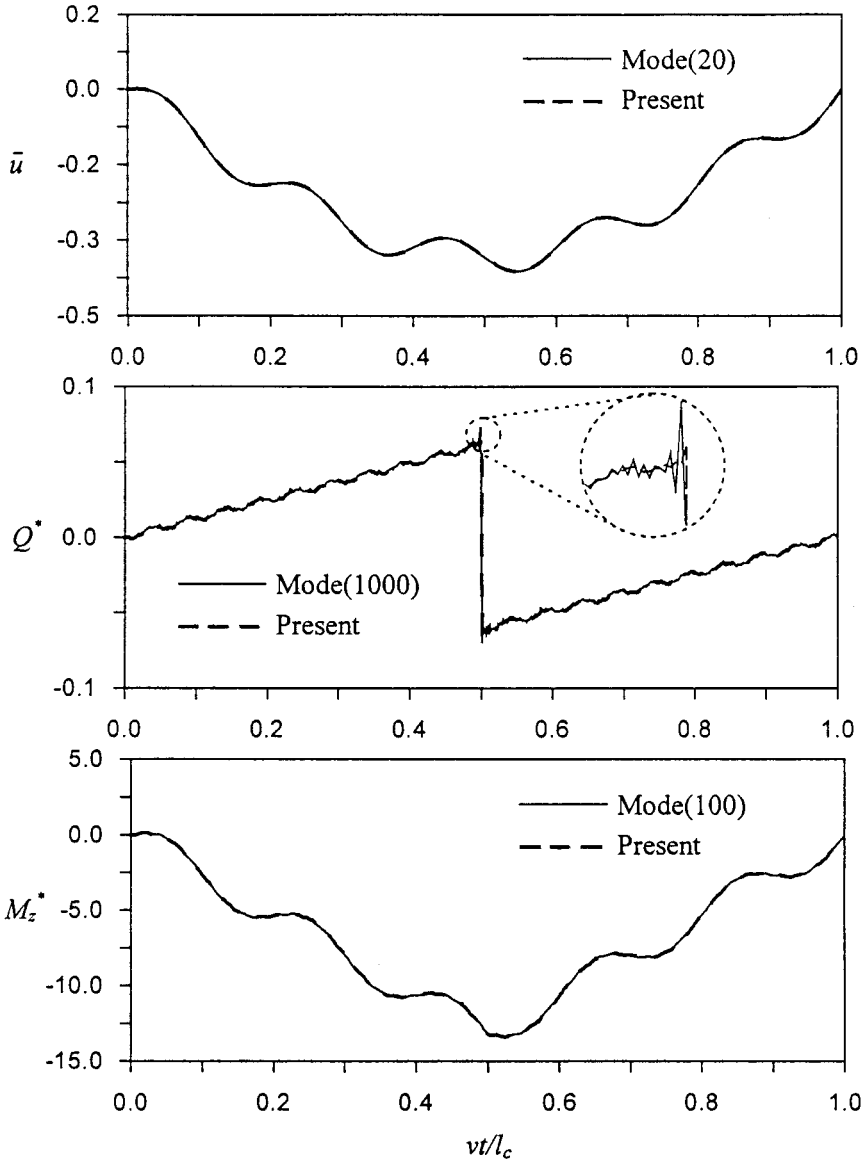

Fig. 6. Comparison of the present solution with a mode superposition solution for a curved beam subjected to a constant moving loading.

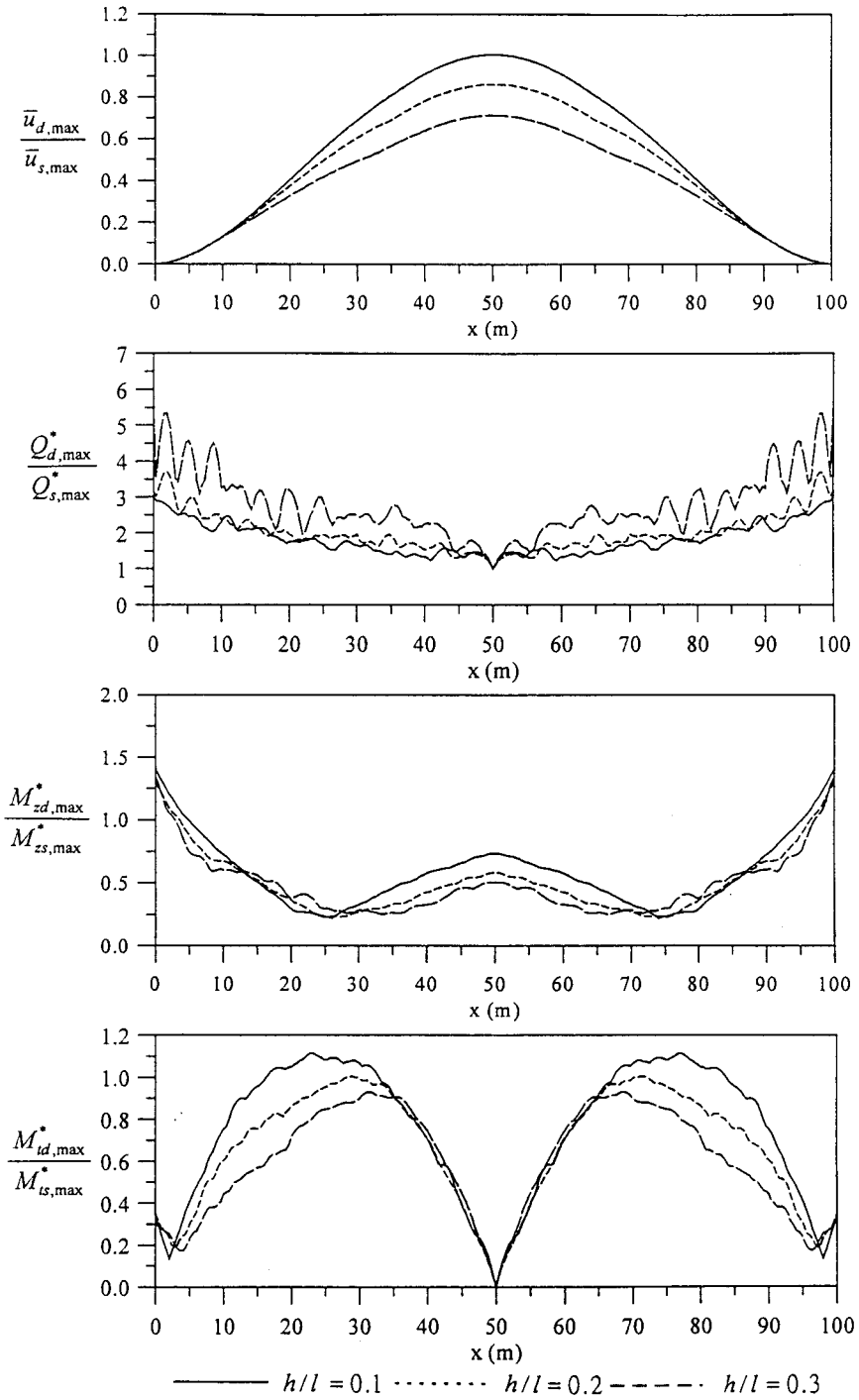

Fig. 7. The ratios of the maximum dynamic response to the maximum static response.

seen, the present results match very well the modal superposition solution. It is worthwhile to mention that the Gibb's phenomenon occurs at the modal superposition solution for shear force, so even 1000 modes could not provide as accurate a solution as the present method does.

5.2. Numerical results

To show the effects of the shape of the curved beam on the dynamic responses, we studied the responses of the parabolic arches prescribed in the section with free vibration where $\eta^* = 0.5$ and $h/l = 0.1$, 0.2, and 0.3, subjected to a rectangular impulse at the middle. The span length l is set equal to 100 m, which is also chosen as the characteristic length of the beam. The material properties for the arches are as follows: Poisson ratio = 0.3 and $\sqrt{E/\rho} = 5000$ m/sec. The first five natural frequencies can be determined from Fig. 4. The impulse loading is described by

$$P(t) = \frac{P_0}{EA_0\bar{\gamma}_0}[U(t-0.1) - U(t-0.2)], \tag{19}$$

where $U(t)$ is the unit step function, and $\frac{P_0}{EA_0\bar{\gamma}_0}$ is taken as 1 in the following numerical results.

Fig. 7 shows the dynamic effect caused by the rectangular impulse on the responses of displacement and stress resultants for parabolic arches with different h/l ratios, in which the vertical axis denotes the ratios of the maximum dynamic responses at different locations on the arch to the maximum static responses. The dynamic effect increases as h/l decreases when the responses for displacement and moments are considered. However, for the shear force response, the opposite trend is seen. From Fig. 7, one can also find that the maximum dynamic response of $\bar{u}$ occurs at the middle while the maximum Q^* and M_z^* occur at the ends. The location for maximum M_t^* changes as h/l changes.

6. Concluding remarks

This paper has presented a systematic and accurate solution for the out-of-plane dynamic responses of curved beams with arbitrary shapes and cross sections by incorporating the dynamic stiffness method with Laplace transform. The dynamic stiffness matrix and equivalent nodal loading vector for curved beams with arbitrary shapes and cross sections have been developed from a series solution using the Frobenius' method. With a simple replacement of the Laplace transform parameter, an exact solution for the free vibration analysis has been established. A convergent solution is always guaranteed either by increasing the solution terms and geometry terms or by increasing the number of elements, so that even the responses of the stress resultants are obtained with very high accuracy but without any numerical difficulty.

The validity of the solution for free vibration analysis has been confirmed through a convergent study with comparison of the present results with the published data. The numerical results for a set of fixed–fixed parabolic arches with a varying cross-section as frequently seen in civil engineering design indicate that the frequency parameters decrease as the ratio of height to span length increases.

The accuracy of the present method for transient response analysis has been demonstrated by comparing it with the modal superposition method based on analysis of a simply-supported circular curved subjected to a moving loading. Excellent agreement has been found between the results from the two methods. Nevertheless, the Gibb's phenomenon has been observed in the modal superposition solution but not in the present solution.

Parabolic arches with a variable cross-section with different rise-to-span ratios have been used to study the effects of shapes on dynamic responses. The dynamic effect of the applied rectangular impulse

at the middle of the parabolic arch on the responses of displacement and moments increases with a decrease of the rise-to-span ratio. However, the opposite trend is observed for the shear force response.

Although the demonstrated examples are quite simple and are single span, the presented solving method can be directly applied to multiple-span curved beams. As a matter of fact, the developed dynamic stiffness matrix and equivalent nodal force vector can be combined with the dynamic stiffness matrixes for other types of elements to accurately analyze the responses of complex systems like arch bridges and space frames with curved members. Furthermore, the present method can also be applied to solve beams with visco–elastic material using the correspondence principle.

Acknowledgements

The research reported herein was supported by the National Science Council, R. O. C. (NSC 87-2211-E-032-015 and NSC 88-2211-E-032-015). Much appreciation is extended to colleagues at the National Center for Research on Earthquake Engineering for valuable discussion.

References

Chang, S.H., 1997. Out-of-plane dynamic analysis for arches of variable cross-section and variable curvature. M.S. thesis, Tamkang University, Taiwan.

Chidamparam, P., Leissa, A.W., 1993. Vibrations of planar curved beams, rings, and arches. Applied Mechanics Reviews 46 (9), 467–483.

Choi, J.K., Lim, J.K., 1993. Simple curved shear beam elements. Communications in Numerical Methods in Engineering 9 (8), 659–669.

Cowper, G.R., 1966. The shear coefficients in Timoshenko's beam theory. Journal of Applied Mechanics 33, 335–340.

Durbin, F., 1974. Numerical inversion of Laplace transforms: an efficient improvement to Dubner and Abate's method. Computer Journal 17, 371–376.

Hildebrand, F.B., 1976. Advanced Calculus for Applications, 2nd ed. Prentice–Hall, Inc, New York.

Hu, J.L., 1988. General Dynamic Analysis of Bridge Structures. Chinese Railroad Publisher, Peking, China.

Huang, C.S., Teng, T.J., Leissa, A.W., 1996. An accurate solution for the in-plane transient response of a circular arch. Journal of Sound and Vibration 196 (5), 595–609.

Huang, C.S., Tseng, Y.P., Chang, S.H., 1998a. Out-of-plane dynamic responses of noncircular curved beams by numerical Laplace transform. Journal of Sound and Vibration 215 (3), 407–424.

Huang, C.S., Tseng, Y.P., Lin, C.R., 1998b. In-plane transient responses of an arch with variable curvature using the dynamic stiffness method with numerical Laplace transform. Journal of Engineering Mechanics, ASCE 124 (8), 826–835.

Huang, C.S., Tseng, Y.P., Leissa, A.W., Nieh, K.Y., 1998c. An exact solution for in-plane vibrations of an arch having variable curvature and cross-section. International Journal of Mechanical Sciences 40 (11), 1159–1173.

Hung, C.L., 1998. Dynamic analysis of non-circular curved beams subjected to moving loading. M.S. thesis, Tamkang University, Taiwan.

Irie, T., Yamada, G., Takashashi, I., 1980a. Out-of-plane vibration of arc bar of variable cross-section. Bulletin of the Japanese Society of Mechanical Engineers 23 (181), 1200–1205.

Irie, T., Yamada, G., Takahashi, I., 1980b. The steady state out-of-plane response of a Timoshenko curved beam with internal damping. Journal of Sound and Vibration 71 (1), 145–156.

Koziey, B.L., Mirza, F.A., 1994. Consistent curved beam element. Computers and Structures 51 (6), 643–654.

Kawakami, M., Sakiyama, T., Matsuda, H., Morita, C., 1995. In-plane and out-of-plane free vibrations of curved beams with variable sections. Journal of Sound and Vibration 187 (3), 381–401.

Laura, P.A.A., Maurizi, M.J., 1987. Recent research on vibrations of arch-type structures. The Shock and Vibration Digest 19 (1), 6–9.

Litewka, P., Rakowski, J., 1997. Efficient curved beam finite element. International Journal for Numerical Methods in Engineering 40 (14), 2629–2652.

Love, A.E.H., 1892. On the vibrations of an elastic circular ring. Proc. Lond. Math. Soc. 24, 118–120.

Markus, S., Nanasi, T., 1981. Vibration of curved beams. The Shock and Vibration Digest 13 (4), 3–14.

Michell, J.H., 1890. The small deformation of curves and surfaces with application to the vibrations of a helix and a circular ring. Messenger of Mathematics 19, 68.

Narayanan, G.V., Beskos, D.E., 1982. Numerical operational methods for time-dependent linear problems. International Journal for Numerical Methods in Engineering 18, 1829–1854.

Rao, S.S., 1971. Effects of transverse shear and rotary inertia on the couple twist–bending vibration of circular rings. Journal of Sound and Vibration 16, 551–566.

Suzuki, K., Kosawada, T., Takahashi, S., 1983. Out-of-plane vibrations of curved bars with varying cross-section. Bulletin of the Japanese Society of Mechanical Engineers 26 (212), 268–275.

Suzuki, K., Sugi, K., Kosawada, T., Takahashi, S., 1986. Out-of-plane impulse response of a curved bar with varying cross-section. Bulletin of the Japanese Society of Mechanical Engineers 29 (258), 4312–4317.

Timoshenko, S.P., Goodier, J.N., 1970. Theory of Elasticity, 3rd ed. McGraw–Hill, New York.

Wagner, H., Ramamurti, V., 1977. Beam vibrations — a review. The Shock and Vibration Digest 9, 17–24.